# Hierarchical Top-down Bottom-up Calibration with Consideration for Uncertainty and Inter-scale Discrepancy of Peierls Stress of bcc Fe

**Aaron E. Tallman[a], Laura P. Swiler[b], Yan Wang[c], David L. McDowell[a, c]**

[a] *School of Materials Science and Engineering, Georgia Institute of Technology, Atlanta, Georgia 30332, USA*

[b] *Optimization and Uncertainty Quantification Department, Sandia National Laboratories, PO Box 5800, MS 1318, Albuquerque, New Mexico 87185, USA*

[c] *GWW School of Mechanical Engineering, Georgia Institute of Technology, Atlanta, Georgia 30332, USA*

## ABSTRACT

A hierarchical multiscale model of plasticity in single crystal bcc Fe, framed at the mesoscale pertaining to a statistically representative set of dislocations for each slip system, relies on specification of a set of parameters which are informed using both bottom-up (atomistic) and top-down (experimental) information. We term this specification process a "connection" between bottom-up and top-down pathways to inform the mesoscale model. The connection is considered in the presence of error, uncertainty, and discrepancy between the models. We expand upon a previously developed reconciled top-down and bottom up calibration method to account for anticipated discrepancy between information from different length scales. The results of a previously formulated likelihood-based connection test of the multiscale model suggest a "missing link" may be responsible for part of the inter-scale discrepancy. In this case, this link is assumed to be a relation between the unit-process (single dislocation line) of coordinated kink-pair nucleation on a screw dislocation segment and the many-body dislocation process which manifests in the onset of experimentally observed plastic deformation in a single crystal. A physics-informed discrepancy layer is formulated to improve the connection in the presence of additional persistent uncertainties. This physics-informed hypothesis testing is

demonstrated as an alternative to fully data-driven search methods, particularly applicable to datasets of limited size that are often encountered in such multiscale material modeling applications. Discrete dislocation dynamics simulations are used to investigate the effect of the Peierls stress on straight screw dislocations and in the operation of Frank-Read sources. Discussion concerns the critical role of uncertainty quantification in providing a basis for this form of incremental hypothesis testing.

## 1 INTRODUCTION

Computational modeling of materials involves simulations at a variety of length and time scales (Andrade et al., 2011; Blanc et al., 2002; Ellis and McDowell, 2017; McDowell, 2010, 2010; Roters et al., 2010). Increasingly, multiple scales of modeling are used in conjunction to capture connections across scales between mechanisms and performance. This is typically approached by using a set of distinct, scale-specific models. The complexity of hierarchical multiscale model (HMM) development suggests that methods for improving plausible models are needed to arrive at suitable multiscale formulations. The development of such HMMs requires inter-scale connections. These connections are made in the presence of uncertainty (Koslowski and Strachan, 2011; Rizzi et al., 2012).

The practice of evaluating a connection in a HMM between top-down (TD) and bottom-up (BU) information pathways is a recent development (Tallman et al., 2017). In the approach, discrepancies in the TD and BU estimates of model parameters which reflect given physical quantities are reconciled through the use of a statistical likelihood framework. The application of the framework in the reconciliation and later evaluation of the TD and BU pathways constitutes an empirical or data-driven method. The method quantifies the average magnitude of the

distances in the parameter domain across which the combined TDBU posterior density is distributed. Reducing this average distance, and thereby the variance in the probabilistic parameter distributions, is necessary to the identifying and refining of connections between scales.

Physical knowledge can be used to refine a connection between length scales. In cases where inconsistencies can be explained through the physical differences between models of a given quantity, the effects of those differences can be quantified and accounted for in the reconciliation process. For instance, in the simulation of yielding in bcc Fe, atomistic predictions and top-down experimental fits of the Peierls stress in a continuum crystal plasticity model differ by a factor of 2 to 3 (Gröger and Vitek, 2007). The difference may be a result of configurations of a network of dislocations which are susceptible to glide at resolved shear stresses in experiments, which can be well below the values determined through atomistic simulations of nucleation of double kinks on a single segment of a screw dislocation using periodic boundary conditions. The influence of many-body dislocation configurations on glide has been further explored with discrete dislocation dynamics (DDD) modeling (Arsenlis et al., 2012).

In this work, a physics-based discrepancy layer is introduced to capture discrepancy between physical descriptions at different scales such that the model calibration based on TD and BU information pathways is improved. It is demonstrated with a crystal plasticity (CP) model, where parameters are calibrated with discrepancy between TD (experimental observations) and BU (atomistic simulations) descriptions. The discrepancy layer is applied to capture the discrepancy between the modeling scales with regard to one of the parameters (thermal slip resistance). DDD simulations are used to illustrate the discrepancy captured. It is shown that the inter-scale discrepancy treatment can improve precision of the inter-scale connection. This

connection refinement, using additional physical considerations and uncertainty quantification to allow for model discrepancy, contrasts with traditional search methods in this application.

## 2   Background

Hierarchical multiscale models (HMM) of materials depend on assumed connections between independently validated models at different length and time scales (McDowell, 2010; Narayanan et al., 2014; Tallman et al., 2017). In a HMM, a mapping between parameters is used to establish this connection. In materials modeling, uncertainty affects any model and thus affects the connections between models (Arendt et al., 2012; Chernatynskiy et al., 2013). The concept of missing physics (Smith, 2013) has been used in model discrepancy approaches (Brynjarsdóttir and O'Hagan, 2014; Ling et al., 2014). In propagation studies, the effects of parametric uncertainties are quantified for the case  where a HMM connection is held fixed (Peherstorfer et al., 2018; Rizzi et al., 2012). The confluence of parameter and model-form uncertainty that arises in HMM connection-making requires multiple distinct and relevant sources of information to disentangle, in addition to a strategy for isolating the connection. Here, hypothesis testing, where a presupposed mechanism is used instead of a best-fit, supports the isolation of connection-effects in this complicated uncertainty condition, where uncertainty of multiple model-forms and parameters must be considered at once.

An estimate of the Peierls stress of a bcc Fe crystal may be approached from both continuum and atomistic scales. In a continuum crystal plasticity model, a Kocks-type activation enthalpy-based flow rule for dislocation glide can be calibrated to experiments (cf. Patra et al., 2014). This flow rule includes the thermal slip resistance as a parameter, whose value reflects the effective level of stress required to activate slip in certain dislocation arrangements present in the

single crystal. Atomistic simulations examine a single screw dislocation exhibiting a coordinated kink-pair nucleation process (Narayanan et al., 2014). The energy barrier at zero applied stress is used to inform predictions of the Peierls stress. In this study, the dissimilarity of the two mechanisms through which the Peierls stress is estimated by either continuum or atomistic treatment is used to refine a connection made between the two pathways for estimation in an empirical sense.

The evaluation of a connection in a HMM is often made under data-scarce conditions. Consequentially, model evaluation techniques that rely on partially withholding data (e.g. cross-validation (Braga-Neto and Dougherty, 2004; Efron and Gong, 1983)) are more challenging to implement. In the case of the current application, omitting a proportion of the available data would result in substantial variations in maximum likelihood estimates of parameters. When data are plentiful, such variations indicate an unreliable model. In data-scarce scenarios, the variations are largely a consequence of the small number of data points. Nevertheless, calibrations and evaluations are needed under data-scarce conditions just as urgently as in the other case, and such conditions are often brought about by virtue of constraints on cost of experiments and/or simulations. This work builds on previous efforts to evaluate a connection under data-scarce conditions by including a model discrepancy layer.

Missing physics is a noteworthy cause of model discrepancy. It can either reflect limitation of a given model form or may reflect a key missing spatial or temporal level in the HMM. In the Bayesian calibration of physics models (Kennedy and O'Hagan, 2001), treatment of model discrepancy is critical to minimizing bias (Brynjarsdóttir and O'Hagan, 2014) and maximizing the identifiability (Ling et al., 2014) of calibration parameters, and is accomplished through including an explicit additive term that adjusts model response or by adjusting

parameters to account for discrepancy (Sargsyan et al., 2015). Discrepancy formulations rely on informative priors to yield results, and in the case of missing physics approaches, the hypothetical impact of those physics is used to provide those informative priors. In the current work, discrepancy between the two length scales is attributed to differences between the analysis of a single dislocation at the atomistic scale and the longer length scale dislocation configurations that give rise to observed experimental behavior in bcc Fe. The formulation of a discrepancy layer is informed by this prior assumption, as opposed to a least-squares fitting. In this work, we examine a discrepancy formulation that involves a mapping between parameters of the BU and TD model, rather than introducing an explicit additive discrepancy correction to the model output.

Separately from model discrepancy methods, various latent variable modeling approaches have been developed to capture hidden causal relationships. These include statistical structural equation modeling (Bentler and Weeks, 1980), Kalman filtering (Meinhold and Singpurwalla, 1983), non-parametric hidden Markov modeling (Gordon et al., 1993), Gaussian process latent variable modeling (Titsias and Lawrence, 2004), causal modeling (Pearl, 2009), and their extensions. Instead of using these approaches to identify the coefficient $C_p$ between TD and BU parameter spaces in Eq. (2), the value of coefficient is obtained from the scaling factor identified by Groger and Vitek (2007), which was derived according to physical knowledge about the mutual interaction between emitted dislocations.

Frank-Read dislocation sources in bcc Fe have been explored (Gröger and Vitek, 2007) for the potential explanation of the Peierls stress and the related discrepancy found between its atomistic predictions and experimentally-informed continuum estimates. To approach this

problem, we appeal to physical arguments that may explain why screw dislocations in networks at mesoscales may activate at applied stress levels much lower than the atomistic estimates of the Peierls barrier. One such mesoscale model of Gröger and Vitek (2007) assumes that mixed character dislocations will glide to form loops within a certain distance of the source. Thereafter, the screw segments which come to dominate the activity of the loops beyond that distance are assumed to glide at resolved stresses below the Peierls stress due to assistance from the stress fields of the mixed character loops in their wake. In order for the Frank-Read source mechanism to operate, the screw segments that form on the first generated dislocation must not prevent the dislocation from completing a glide loop. In this work, DDD simulations are performed to examine the Frank-Read source as a mesoscopic explanation of discrepancy in the Peierls stress between scales.

DDD simulations allow a variety of dislocation configurations to be examined (Amodeo and Ghoniem, 1990; Sobie et al., 2017a, 2017b). In this work, the simulations are used to investigate the two dislocation structure idealizations relevant to the scale discrepancy argument of Gröger and Vitek (2007). These include a simulation of periodic parallel straight screw dislocations and a simulation of periodically placed Frank-Read sources. The high atomistic prediction of Peierls stress for screw segments is included in the simulations. An in-depth DDD study of this problem is left to future work, as the intent here is to explain the concept of the discrepancy layer.

## 3    Methodology

The previously used top-down (TD) and bottom-up (BU) likelihood functions are augmented with an inter-scale discrepancy layer. In this section, the likelihood functions are

described and the inter-scale discrepancy is formulated. The data from TD and BU are combined using the method of reconciliation previously detailed (Tallman et al., 2017), which multiplicatively combines surrogate model-based TD likelihood functions and BU penalty functions of Gaussian form to inform a TDBU posterior for parameters. In the TDBU calibration approach, a standard likelihood formulation for the top-down model (or its surrogate) is multiplied by a function which penalizes large differences between BU and TD parameters. The total likelihood represents how much the top down calibration process is informed and influenced by bottom up parameters. Thus, it is not a direct combination of TD and BU data but an updating of TD data by how much information the BU parameters bring to the TD calibration. A brief summary of the method is provided here.

Data from experiments on the temperature and crystallographic loading orientation dependent stress-strain behavior of single crystal bcc Fe (Keh, 1965; Spitzig and Keh, 1970) are gathered. The yield strength (proportional limit) is identified in the experimental data for use in calibrating a set of parameters of the flow rule, i.e.,

$$\dot{\gamma}^{\alpha} = \begin{cases} \dot{\gamma}_0 \exp\left( -\dfrac{\Delta F_g}{kT} \left( 1 - \left( \dfrac{\tau_f^{\alpha} - s_a^{\alpha}}{s_t^{\alpha}} \right)^p \right)^q \right); & \text{for } \tau_f^{\alpha} > s_a^{\alpha} \\ 0; & \text{for } \tau_f^{\alpha} \leq s_a^{\alpha} \end{cases} \tag{1}$$

in a crystal plasticity model, where $\dot{\gamma}^{\alpha}$ is the crystallographic shearing rate on slip system $\alpha$, $\dot{\gamma}_0$ is the pre-exponential factor, $\Delta F_g$ is the activation enthalpy of thermally activated dislocation glide at zero resolved shear stress, $\tau_f^{\alpha}$ is the driving force on the slip system which includes non-

Schmid stresses, $s_a^\alpha$ is the athermal resistance to slip, $s_t^\alpha$ is the thermal resistance to slip, and $p$ and $q$ are shape parameters.

The CP model is executed for a set of values for each calibration parameter. A set of second-order polynomial regression models is used to interpolate across the calibration parameter space. Each of these models defines a relationship between calibration parameters and the predicted yield strength of the CP model at a specific temperature and crystallographic orientation, i.e.,

$$f_i\left(\theta_1,\cdots,\theta_{N_\theta}\right) = \alpha_0 + \sum_{j=1}^{N_\theta} \alpha_j\theta_j + \sum_{j=1}^{N_\theta}\sum_{k=j}^{N_\theta} \alpha_{N_\theta-1+j+k}\theta_k\theta_j, \text{ for } T_i, g_i \tag{2}$$

where $\alpha$ are regressive coefficients, $\theta$ are calibration parameters, $T_i$ is the i-th temperature, and $g_i$ is the i-th orientation of i experimental observations of the response. Through a standard sum of squared errors comparison with the experimental values of yield strength, likelihood functions are generated in terms of the calibration parameters. These likelihood functions are used as the basis of TD information in calibration parameter space. The BU information is contained in a reference estimate of parameters, labeled as 'reference' to signify that the estimate originates externally to the model being calibrated. The reference estimate is used to inform some penalty functions in a form which can be combined with the TD likelihood functions.

The new model discrepancy layer changes the relationship between the BU and TD parameter spaces. In the previous study, the TD and BU parameter spaces were defined as identical; in other words, the same set of mesoscale CP model parameters were estimated via information from both BU and TD pathways. In the present study, the additional information

9

involving discrepancy relates to the Peierls stress alone; accordingly, the model discrepancy layer here is demonstrated with a single parameter: the thermal slip resistance, $s_t$. A linear relation between the BU and TD parameter spaces is defined as

$$s_{t,BU} = C_p \ s_{t,TD} \tag{3}$$

where $s_{t,BU}$ is the BU-defined thermal slip resistance and $s_{t,TD}$ is the TD-defined thermal slip resistance.

The value $C_p = 2$ is taken from the calculations of Gröger and Vitek (2007) of the stress barrier for dislocation glide in a configuration of Frank-Read sources at a dislocation density of the order of $10^{12} \, \mathrm{m}^{-2}$. Their calculations, based in the isotropic elastic theory of dislocations, reflect the effects of interactions of Frank-Read emissions on the effective barrier to dislocation glide. While the Peierls barrier of screw dislocations is unchanged, the configuration of dislocations allows glide to occur at a steady state, at resolved shear stresses of one half the Peierls barrier of screw dislocations. The annihilation of emitted dislocations occurs at a given radius from the Frank-Read sources (which depends on dislocation density). Dislocations are emitted as mixed character and are assumed to become pure screw after gliding for some distance. If there exist $N_s$ screw dislocations at distances $x_i$ from a source and $N_m$ mixed character dislocations at distances $y_k < x_i \forall i$ the $i$-th screw dislocation will glide when

$$\sigma_a + \frac{\mu b}{2\pi} \sum_{\substack{j=1 \\ j \neq i}}^{N_s} \frac{1}{x_i - x_j} + \frac{\mu b}{2\pi\alpha} \sum_{k=1}^{N_m} \frac{1}{x_i - y_k} + \frac{\mu b}{2\pi\alpha} \frac{1}{x_i} \geq \sigma_P \tag{4}$$

where $\sigma_a$ is the applied stress, $\sigma_P$ is the Peierls barrier of screw $b$ is the Burgers vector of the emitted dislocations, $\mu$ is the shear modulus, and $\alpha$ is a constant. The stress exerted by the mixed character dislocations on the screw dislocations allows the Frank-Read source to be active at applied stressed below $\sigma_P$. The value $C_p = 2$ taken in this work corresponds to one of many dislocation densities and source spacings considered in the work of Gröger and Vitek (2007).

In the HMM formulation, the value $C_p = 2$ is intended to account for the difference in the Peierls stress levels, between the prediction from atomistic simulations (Narayanan et al., 2014) of purely screw character dislocations, as high as 1000 MPa, and the effective value gathered from experimental observations (Keh, 1965; Patra et al., 2014) which governs larger patterns of dislocations, as low as 390 MPa. The other four parameters ($\dot{\gamma}^\alpha$, $\Delta F_g$, $p$, and $q$) remain identical in the calibration set from BU to TD. Given the fixed nature of the relationship that we assume from Eq. 2, the rest of our analysis considers the improvement to the TDBU calibration rendered by this discrepancy approach. After the adjustment, the remaining steps of the TDBU reconciliation are executed.

The likelihood functions are combined multiplicatively with the penalty functions in a constrained likelihood function (CLF). The addition of the discrepancy layer forces the decision of which parameter basis (TD, BU, or another) to use to formulate the CLF. The maximum likelihood estimate is unaffected by the choice; however, the inferred values of parameter uncertainty based on the CLF will vary. The uncertainty estimates are calculated in terms of calibration parameters normalized to intervals, i.e., $[0,1]$. This prevents the units of the parameters from influencing outcomes. However, it also leads to a situation where the results depend on the values chosen to determine admissible parameter ranges. Given that the goal of

this study is to determine if a physics-informed discrepancy layer is sufficient to allow a connection to be made between TD and BU data, it is appropriate to maintain consistent admissible ranges to make such a comparison.

The connection test is performed for the model which includes the discrepancy layer. In the formulation of this test, the discrepancy layer adjusts the BU reference parameter estimate which is incorporated in the calculation of TDBU parameter uncertainty. The difference in the parameter values is shown in Table 1. The original BU values are used in both cases and are translated into a TD native basis using Eq. (2) in the case of the discrepancy inclusive approach. In the approach without discrepancy, the TD basis is arrived at using a one-to-one correspondence.

Table 1. The original and discrepancy adjusted reference estimates used as the BU penalty.

| $\hat{\boldsymbol{\theta}}_{BU}^{ref}$ | $\dot{\gamma}_0$ | $\Delta F_g$ | $p$ | $q$ | $s_t$ |
|---|---|---|---|---|---|
| Original | $3.19 \times 10^7 s^{-1}$ | 0.57 eV | 0.67 | 1.18 | 1040 MPa |
| Discrepancy Adjusted | $3.19 \times 10^7 s^{-1}$ | 0.57 eV | 0.67 | 1.18 | 520 MPa |

The TDBU calibration method requires evaluations of the uncertainty in TD information through an experimental variance term, $\sigma_{\exp}^2$ for each data point and the uncertainty in BU information through the variance of the penalty, $\sigma_p^2$. Both of these parameters influence the results of a connection test, as the test checks for uncertainty reduction, and a lower uncertainty level in inputs leads to a smaller tolerance for mismatch in data sources. In the extreme case,

fully certain TD observations mean that new BU data do not add additional information or value. This sensitivity to input uncertainties, as is common in Bayesian methods, is a useful capacity of the method. Given that not all data are accompanied by uncertainty estimates, additional effort may be needed to ensure the test results appropriately reflect the available information. The connection test involves quantifying the cost and benefit of using BU information to inform the TD parameters. The connection may be very helpful or may be not helpful at all (e.g. the TD and BU parameters conflict or completely disagree with each other).

Here, a summary of the connection test is given, which is described in more detail elsewhere (Tallman et al., 2017). The BU penalty functions and TD likelihood functions are included in a constrained likelihood function (CLF). This CLF is raised to an exponent, the value of which is informed using the assumed cost of the connection, $u$. A value of $u = 1$ reflects no connection cost where the TD and BU data agree, and a value of $u = 0$ reflects an infinite connection cost, where complete disagreement exists between the TD and BU data. The result is normalized to satisfy the law of total probability over the admissible parameter space to give a probability density function (PDF) in the parameter space. A quadrature-based Bayesian approach is used to calculate the $\text{PDF}(\boldsymbol{\theta})$. The calibration variance is calculated by finding the square Euclidean distance of the PDF from the centroid of the PDF. These equations are given in Table 2.

Table 2. Equations defining the terms of the TDBU connection test.

| | |
|---|---|
| $$Penalty\left(\hat{\mathbf{\theta}}\right)=\sum_{i}^{\hat{\theta} in \hat{\mathbf{\theta}}}\left(\frac{\hat{\theta}_i - \theta_{i,ref}}{\sigma_p}\right)^2,$$ $$SSE\left(\mathbf{\theta}\right)=\sum_{j=1}^{Data}\frac{\left(f_j\left(\mathbf{\theta}\right)-Y^E\left(\mathbf{x}_j\right)\right)^2}{\sigma_{exp,j}^2}$$ | Penalty functions and sum square error calculations using surrogates $f_j$ in place of CP model, physical parameter value $\mathbf{x}$ at data point $j$, experimental response $Y^E$ |
| $$CLF\left(\mathbf{\theta}\right)=\exp\left[-\frac{1}{2}\left(Penalty\left(\mathbf{\theta}\right)+SSE\left(\mathbf{\theta}\right)\right)\right]$$ | Constrained Likelihood Function |
| $$u=\frac{1}{SSE\left(\hat{\mathbf{\theta}}\right)+Penalty\left(\hat{\mathbf{\theta}}\right)}$$ | Connection cost $u$ is evaluated at the maximum likelihood estimate, $\hat{\mathbf{\theta}}$ |
| $$PDF\left(\mathbf{\theta}\right)=Const.\times\exp\left[-\frac{u}{2}\left(Penalty\left(\mathbf{\theta}\right)+SSE\left(\mathbf{\theta}\right)\right)\right]$$ | Probability density function |
| $$\sigma_\theta^2=\int_{\mathbf{\theta}_{min}}^{\mathbf{\theta}_{max}}PDF\left(\mathbf{\theta}\right)Dist^2\left(\mathbf{\theta},\bar{\mathbf{\theta}}\right)d\mathbf{\theta}$$ | Calibration variance $\sigma_\theta^2$ evaluated from centroid of parameter space, $\bar{\mathbf{\theta}}$ |

DDD simulations were pursued to provide a mechanistic description of the scale discrepancy layer introduced in this work. The DDD simulations are performed using a fast-Fourier transform accelerated DDD code (Bertin et al., 2015). Edge dislocations in bcc Fe have been shown to be highly mobile at low applied stresses (Monnet and Terentyev, 2009). The simulations assign the Peierls stress to be 1 GPa for screw dislocation segments, consistent with atomistic modeling results, and 10 MPa for edge and mixed character dislocation segments. An overdamped mobility law is used for all dislocation segments. The simulations are carried out

using periodic boundary conditions. Shear stress is applied at three levels: the stress at which a straight screw dislocation begins to glide (here 1 GPa), 75% (750 MPa), and 50% of that stress (500 MPa). The simulation volume is a cube of 10,000 unit cells in length (2.87 $\mu$m). A Frank-Read source of width 160 nm is assumed.

The DDD simulations of a Frank-Read source are carried out using a prismatic dislocation loop. The glissile portions of the loop are initially pure edge dislocation segments on $\frac{1}{2}\langle 111 \rangle \{110\}$ slip systems. As a result, these segments are initially highly mobile under resolved shear stress. The simulations are carried out to examine whether or not the screw segments which form as the dislocation bows out will inhibit the formation of glide loops. This step is identified as critical to the feasibility of the explanation provided by Gröger and Vitek (2007).

## 4    Results

The impact of the discrepancy layer is evaluated in this section. To provide a point of comparison, the uncertainty estimates made in previous work without a model discrepancy treatment are included (Tallman et al., 2017). As mentioned above, DDD simulations of a Frank-Read source in bcc Fe are also included to highlight the assumptions which underlie the mechanistic description of the scale discrepancy used to motivate this work.

The parameter $\sigma_p$ in the penalty function (listed in Table 2) controls the influence of the BU information on the probability density of the calibration parameters. As a result, the comparison of the variance of the TDBU calibration and the TD calibration depends strongly on

15

the value of $\sigma_p$. In Figure 1, the calibration variance $\sigma_\theta^2$ is shown as a function of $\sigma_p$ for both connection formulations considered in this work. The calibration variance is a monotonic function for the case of TDBU with the discrepancy layer, decreasing as BU information is included. For the TDBU without the discrepancy layer, the parameter uncertainty increases as BU information is included, up until the BU information begins to outweigh the TD information (at $\sigma_p$ values < 0.1).
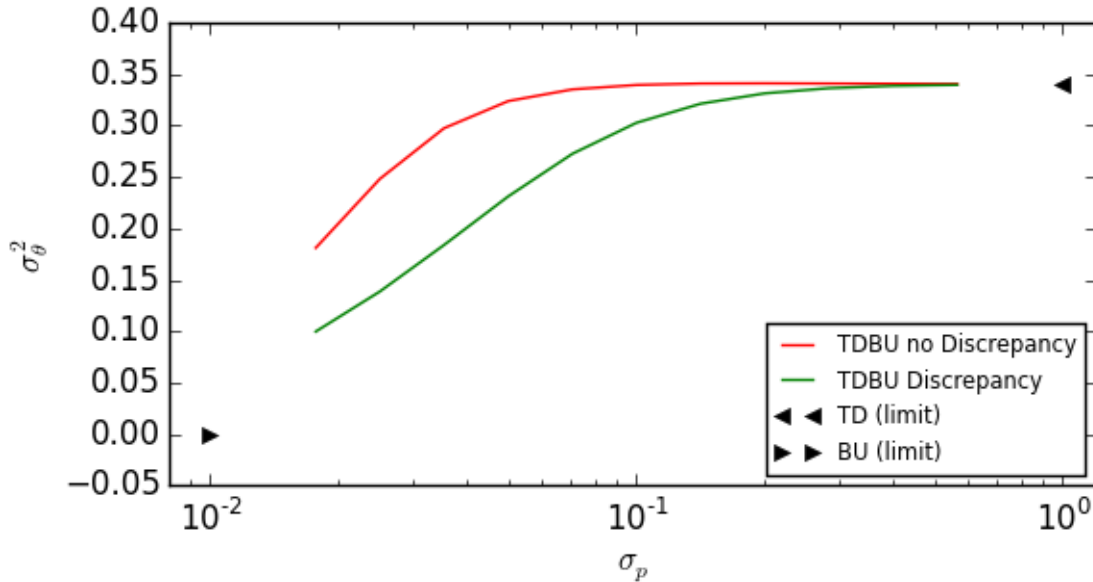


Figure 1. Plot of the calibration variance as function of the penalty parameter. Limits are plotted for context.

DDD simulations were carried out at 3 applied shear stress levels, 1000, 750, and 500 MPa. The limited mobility of screw dislocation segments is observed to control the operation of the Frank-Read source. Snapshots of the dislocation lines are taken normal to the glide plane at arbitrary times during the simulations to highlight the mechanism present at each stress level. These images are included in Figure 2. The dislocation line in Figure 2a continues to bow out, but the applied stress does not drive screw segments to glide. In Figures 2b and 2c, the applied

stress is sufficiently high to cause screw segments to glide such that the Frank-Read source may generate glide loops. In Figure 2c, the screw dislocations are generated as a result of the glide loops annihilating at the periodic boundary in the direction of the edge dislocation motion. These screw dislocations were able to glide as necessary for the Frank-Read source to operate, however the simulation was not continued long enough to approach conditions of source saturation. Still, they illustrate the key point of the mesoscopic configuration controlling the effective value of the lattice resistance that one would interpret from experiments based on operation of distributed Frank-Read sources. The results support the discrepancy layer assignment $C_p = 2$ in Eq. (2) qualitatively if not quantitatively.
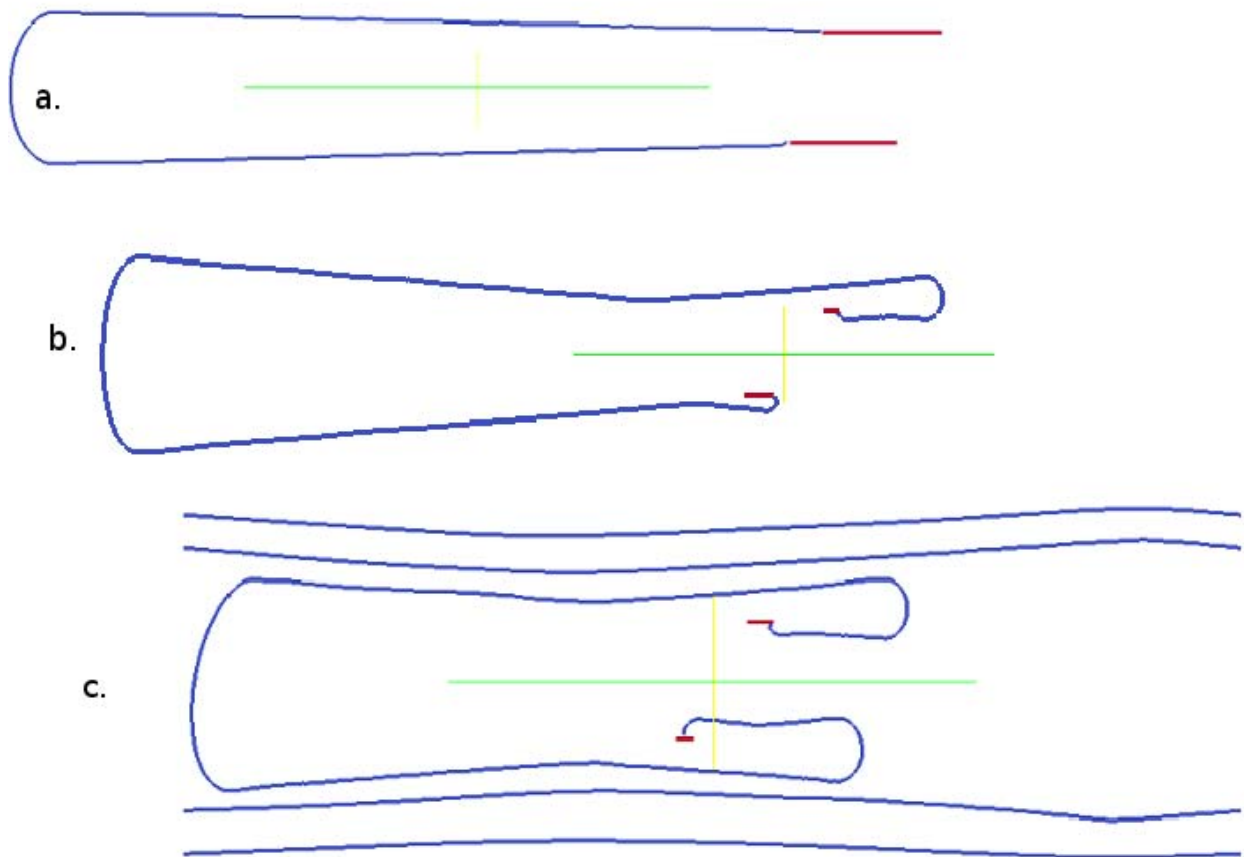


Figure 2. Snapshots of DDD simulations of Frank-Read sources under applied shear stress of 500 MPa (a.), 750 MPa (b.), and 1000 MPa (c.).

# 5    Discussion

The benefits of the discrepancy layer are discussed. The dislocation configurations which allow a reduction in the thermal resistance to slip in bcc Fe are explored in this section. Additionally, the difficulty of adjusting connections in HMMs without informative prior estimates is addressed. Atomistic modeling which would increase the precision of predictions is suggested.

The addition of the discrepancy layer allows for the BU information to contribute to a reduction of uncertainty in the HMM. In previous work (Tallman et al., 2017), the combination of TD and BU information was concluded to increase uncertainty, once connection cost was considered. Here, the discrepancy layer allows for a reconciliation of TD and BU information which amounts to a reduction of the parametric uncertainty, as seen in Figure 1. At the preferred value of $\sigma_p = 0.1$, the value for the TDBU uncertainty estimate, $\sigma^2_{\theta,\mathrm{TDBU}} = 0.30$, is a reduction from the TD only estimate, $\sigma^2_{\theta,\mathrm{TD}} = 0.34$. The interpretation of this result follows.

The immediate result of the including the discrepancy layer is to achieve a connection which adds mesoscale information to the calibration of the HMM. This result is predicated on the uncertainty of each data source (TD via $\sigma^2_{\mathrm{exp}}$ and BU via $\sigma^2_p$). As more data or more reliable data become available, the initial uncertainties associated with the TD-only and BU-only calibrations may reduce. The surrogate model used to define likelihood functions in parameter space might lead to reductions in initial uncertainty. All of these reductions make further reductions to uncertainty from a TDBU calibration more difficult. In other words, as the model improves, the connection must also improve to continue to be of value.

A longer-term result is the suggested importance of the discrepancy between the atomistic parameter estimates and the continuum values in HMM development. This is to say that more investigation may return analogous discrepancy formulations for other parameters in the original TDBU calibration parameter set, further reducing uncertainty in connections. Furthermore, the development of HMM connections can be incremental and driven by the TDBU connection test. The framework proposed here helps to guide the modeler to seek specific arguments and mechanisms for discrepancy to improve the BU and TD model connection, so it very much resides in the realm of physics-based modeling.

The choice of connection basis parameters is not resolved in this study. The example shown used the TD parameters as a basis to allow the admissible parameter space to remain consistent with a comparison case. The complication arising from adjusting the admissible parameter space is that, in addition to providing a finite space for parameter calibration, the admissible parameter space also provides a means of normalizing the magnitude of variations in parameter values. To allow for comparisons of information connection scenarios which support different admissible parameter ranges, or even different parameter spaces, a different normalization scheme is needed. To provide a consistent basis for evaluating parameter variations, independent of units, a basis can be made in a model of effects, i.e., the size of a parameter value change is considered relative to a change incurred in a quantity of interest (QoI) which is some function of the parameters, the model response, or a combination thereof. An example is made using model response as the QoI. The unit of normalization is approximated

$$\theta_{norm} \simeq E\left[\frac{\Delta\theta}{\Delta Y}\right] \text{ for all } \theta \text{ in } \left[\boldsymbol{\theta}_{min}, \boldsymbol{\theta}_{max}\right] \tag{5}$$

where $\theta_{norm}$ is the normalizing value for calibration parameter $\theta$, and $Y$ is the model response. By normalizing changes in parameters to measured effects, the assumption that changes in parameters have magnitudes relative to the admissible ranges may be relaxed.

In cases where different parameter sets are considered, an approach to make a like comparison may require the consideration of the effects of each parameter in terms of similarity. In this case, a QoI with at least as many dimensions as parameters is best. Taken at some representative number of points in parameter space, the similarity of effects is calculated as

$$Sim(\theta_1, \theta_2) = \frac{1}{\left\| \Delta \mathbf{Y}^2 \right\|} \frac{\Delta \mathbf{Y}}{\Delta \theta_1} \cdot \frac{\Delta \mathbf{Y}}{\Delta \theta_2} \tag{6}$$

where the similarity value ranges from 0 to 1. The application of the TDBU calibration to connections between parameter spaces of different shapes and sizes is left to future work.

The DDD simulations were carried out at very low effective dislocation densities ($\sim 3 \times 10^{10} \, \text{m}^{-2}$). At higher dislocation densities, the attraction between dislocation dipoles would contribute and assist sessile segments in gliding. This suggests that the Frank-Read source explanation of the Peierls stress discrepancy is likely to be plausible at realistic dislocation densities (greater than $1 \times 10^{12}$), where dislocations may find sinks, despite the lack of activity shown in the DDD simulations of this work at lower applied stress (500 MPa). An investigation of the Frank-Read source within more realistic microstructures is left to future work.

There is need for atomistic investigation of stress-dependent mobility of mixed character dislocations in bcc Fe. The Frank-Read source was shown in this work to be able to operate

under an applied stress of 75% of the Peierls stress of screw dislocations. To refine this determination further, atomistic simulations will be needed. The DDD simulations rely upon the tangent vector of each dislocation segment to determine screw/edge character. As a result, the glide of the screw segments which occurred due to the propagation of mixed character regions of the dislocation line along screw segments was highly dependent on the angles (between the dislocation line and the Burgers vector) at which a segment was considered a screw segment. The DDD code is not atomistic, and hence cannot explicitly describe atomistic mechanisms such as kink-pair nucleation; such information is heuristically introduced in the segment mobility functions. The contribution of DDD simulations here is to match behavior as exhibited by dislocations. To provide more accuracy in predicting the relation of the effective Peierls barrier to Frank-Read sources to the Peierls stress of pure screw dislocations, atomistic simulations of glide loops will be necessary at larger scale such that the DDD code can be made to match the behavior shown in atomistic simulation.

The discrepancy relation has explored physics-based calculations to restrict flexibility in the method. The presence of discrepancy in TD and BU information would be trivial to deal with if a discrepancy layer was allowed to modify the BU parameter space such that $\hat{\theta}_{BU} = \hat{\theta}_{TD}$. The arguments against this practice is that such a treatment has no understanding to impart to the modeler, and renders the information from BU to be without impact on the calibration itself. On the contrary, the method employed here used a connection test to determine that a specific multibody explanation of discrepancy in atomistic and continuum predictions of Peierls stress in bcc Fe is sufficient to reconcile the BU and TD information in the current HMM.

## ACKNOWLEDGEMENTS

## REFERENCES

Amodeo, R.J., Ghoniem, N.M., 1990. Dislocation dynamics. II. Applications to the formation of persistent slip bands, planar arrays, and dislocation cells. Phys. Rev. B 41, 6968–6976. https://doi.org/10.1103/PhysRevB.41.6968

Andrade, J.E., Avila, C.F., Hall, S.A., Lenoir, N., Viggiani, G., 2011. Multiscale modeling and characterization of granular matter: From grain kinematics to continuum mechanics. J. Mech. Phys. Solids 59, 237–250. https://doi.org/10.1016/j.jmps.2010.10.009

Arendt, P.D., Apley, D.W., Chen, W., 2012. Quantification of Model Uncertainty: Calibration, Model Discrepancy, and Identifiability. J. Mech. Des. 134, 100908. https://doi.org/10.1115/1.4007390

Arsenlis, A., Rhee, M., Hommes, G., Cook, R., Marian, J., 2012. A dislocation dynamics study of the transition from homogeneous to heterogeneous deformation in irradiated body-centered cubic iron. Acta Mater. 60, 3748–3757. https://doi.org/10.1016/j.actamat.2012.03.041

Bertin, N., Upadhyay, M.V., Pradalier, C., Capolungo, L., 2015. A FFT-based formulation for efficient mechanical fields computation in isotropic and anisotropic periodic discrete dislocation dynamics. Model. Simul. Mater. Sci. Eng. 23, 065009. https://doi.org/10.1088/0965-0393/23/6/065009

Blanc, X., Bris, C.L., Lions, P.-L., 2002. From Molecular Models¶to Continuum Mechanics. Arch. Ration. Mech. Anal. 164, 341–381. https://doi.org/10.1007/s00205-002-0218-5

Brynjarsdóttir, J., O'Hagan, A., 2014. Learning about physical parameters: the importance of model discrepancy. Inverse Probl. 30, 114007. https://doi.org/10.1088/0266-5611/30/11/114007

Chernatynskiy, A., Phillpot, S.R., LeSar, R., 2013. Uncertainty Quantification in Multiscale Simulation of Materials: A Prospective. Annu. Rev. Mater. Res. 43, 157–182. https://doi.org/10.1146/annurev-matsci-071312-121708

Ellis, B.D., McDowell, D.L., 2017. Application-Specific Computational Materials Design via Multiscale Modeling and the Inductive Design Exploration Method (IDEM). Integrating Mater. Manuf. Innov. 6, 9–35. https://doi.org/10.1007/s40192-017-0086-3

Gröger, R., Vitek, V., 2007. Explanation of the discrepancy between the measured and atomistically calculated yield stresses in body-centred cubic metals. Philos. Mag. Lett. 87, 113–120. https://doi.org/10.1080/09500830601158781

Keh, A.S., 1965. Work hardening and deformation sub-structure in iron single crystals deformed in tension at 298°k. Philos. Mag. 12, 9–30. https://doi.org/10.1080/14786436508224942

Kennedy, M.C., O'Hagan, A., 2001. Bayesian calibration of computer models. J. R. Stat. Soc. Ser. B Stat. Methodol. 63, 425–464. https://doi.org/10.1111/1467-9868.00294

Koslowski, M., Strachan, A., 2011. Uncertainty propagation in a multiscale model of nanocrystalline plasticity. Reliab. Eng. Syst. Saf. 96, 1161–1170. https://doi.org/10.1016/j.ress.2010.11.011

Ling, Y., Mullins, J., Mahadevan, S., 2014. Selection of model discrepancy priors in Bayesian calibration. J. Comput. Phys. 276, 665–680. https://doi.org/10.1016/j.jcp.2014.08.005

McDowell, D.L., 2010. A perspective on trends in multiscale plasticity. Int. J. Plast., Special Issue In Honor of David L. McDowell 26, 1280–1309. https://doi.org/10.1016/j.ijplas.2010.02.008

Monnet, G., Terentyev, D., 2009. Structure and mobility of the $\frac{1}{2}\langle 111\rangle\{112\}$ edge dislocation in BCC iron studied by molecular dynamics. Acta Mater. 57, 1416–1426. https://doi.org/10.1016/j.actamat.2008.11.030

Narayanan, S., McDowell, D.L., Zhu, T., 2014. Crystal plasticity model for BCC iron atomistically informed by kinetics of correlated kinkpair nucleation on screw dislocation. J. Mech. Phys. Solids 65, 54–68. https://doi.org/10.1016/j.jmps.2014.01.004

Patra, A., Zhu, T., McDowell, D.L., 2014. Constitutive equations for modeling non-Schmid effects in single crystal bcc-Fe at low and ambient temperatures. Int. J. Plast. 59, 1–14. https://doi.org/10.1016/j.ijplas.2014.03.016

Peherstorfer, B., Willcox, K., Gunzburger, M., 2018. Survey of Multifidelity Methods in Uncertainty Propagation, Inference, and Optimization. SIAM Rev. 60, 550–591. https://doi.org/10.1137/16M1082469

Rizzi, F., Najm, H., Debusschere, B., Sargsyan, K., Salloum, M., Adalsteinsson, H., Knio, O., 2012. Uncertainty Quantification in MD Simulations. Part I: Forward Propagation. Multiscale Model. Simul. 10, 1428–1459. https://doi.org/10.1137/110853169

Roters, F., Eisenlohr, P., Hantcherli, L., Tjahjanto, D.D., Bieler, T.R., Raabe, D., 2010. Overview of constitutive laws, kinematics, homogenization and multiscale methods in crystal plasticity finite-element modeling: Theory, experiments, applications. Acta Mater. 58, 1152–1211. https://doi.org/10.1016/j.actamat.2009.10.058

Sargsyan, K., Najm, H.N., Ghanem, R., 2015. On the Statistical Calibration of Physical Models. Int. J. Chem. Kinet. 47, 246–276. https://doi.org/10.1002/kin.20906

Smith, R.C., 2013. Uncertainty Quantification: Theory, Implementation, and Applications. SIAM-Society for Industrial and Applied Mathematics, Philadelphia.

Sobie, C., Capolungo, L., McDowell, D.L., Martinez, E., 2017a. Modal analysis of dislocation vibration and reaction attempt frequency. Acta Mater. 134, 203–210. https://doi.org/10.1016/j.actamat.2017.02.005

Sobie, C., Capolungo, L., McDowell, D.L., Martinez, E., 2017b. Scale transition using dislocation dynamics and the nudged elastic band method. J. Mech. Phys. Solids 105, 161–178. https://doi.org/10.1016/j.jmps.2017.05.004

Spitzig, W.A., Keh, A.S., 1970. Orientation and temperature dependence of slip in iron single crystals. Metall. Trans. 1, 2751–2757. https://doi.org/10.1007/BF03037811

Tallman, A.E., Swiler, L.P., Wang, Y., McDowell, D.L., 2017. Reconciled Top-down and Bottom-up Hierarchical Multiscale Calibration of bcc Fe Crystal Plasticity. Int. J. Multiscale Comput. Eng. 15. https://doi.org/10.1615/IntJMultCompEng.2017021859